Chemistry & Biology
Article

Inositol Hexakisphosphate Kinase Products Contain Diphosphate and Triphosphate Groups

Petra Draškovič,[1] Adolfo Saiardi,[2] Rashna Bhandari,[3] Adam Burton,[2] Gregor Ilc,[4] Miroslav Kovačevič,[5] Solomon H. Snyder,[3] and Marjetka Podobnik[1,*]
[1]Department of Biosynthesis and Biotransformation, National Institute of Chemistry, Hajdrihova 19, 1000 Ljubljana, Slovenia
[2]Medical Research Council Laboratory for Molecular Cell Biology and Cell Biology Unit, University College London, Gower Street, London WC1E 6BT, United Kingdom
[3]Department of Neuroscience, Johns Hopkins University, School of Medicine, 725 North Wolfe Street, Baltimore, MD 21205, USA
[4]Slovenian NMR Center
[5]Department of Analytical Chemistry
National Institute of Chemistry, Hajdrihova 19, 1000 Ljubljana, Slovenia
*Correspondence: marjetka.podobnik@ki.si
DOI 10.1016/j.chembiol.2008.01.011

SUMMARY

Eukaryotic cells produce a family of diverse inositol polyphosphates (IPs) containing pyrophosphate bonds. Inositol pyrophosphates have been linked to a wide range of cellular functions, and there is growing evidence that they act as second messengers. Inositol hexakisphosphate kinase (IP6K) is able to convert the natural substrates inositol pentakisphosphate (IP_5) and inositol hexakisphosphate (IP_6) to several products with an increasing number of phospho-anhydride bonds. In this study, we structurally analyzed IPs synthesized by three mammalian isoforms of IP6K from IP_5 and IP_6. The NMR and mass analyses showed a number of products with diverse, yet specific, stereochemistry, defined by the architecture of IP6K's active site. We now report that IP6K synthesizes both pyrophosphate (diphospho) as well as triphospho groups on the inositol ring. All three IP6K isoforms share the same activities both in vitro and in vivo.

INTRODUCTION

The inositol ring offers an energetically stable base for the formation of a great variety of phosphorylated inositol derivatives. Among nine possible isomers, the *myo* configuration of inositol is the most widespread and versatile in biological systems (reviewed in Irvine and Schell, 2001; Michell, 2007). Although the importance of the inositol trisphosphate (1,4,5)IP_3 as a Ca^{2+}-mobilizing second messenger was demonstrated in the early 1980s (Streb et al., 1983), the first direct observations of inositol polyphosphates (IPs) containing diphosphate or pyrophosphate groups were made in the early 1990s (Menniti et al., 1993a; Stephens et al., 1993; Glennon and Shears, 1993). The distinctive features of these inositol pyrophosphates (PP-IPs) are their rapid turnover through coupled kinase/phosphatase cycles (Menniti et al., 1993a, 1993b), and the high energy of the pyrophosphate bonds (Stephens et al., 1993; Hand and Honek, 2007), suggesting their importance in cell physiology and metabolism. PP-IPs manifest several functions: regulating DNA recombination, telomere length maintenance, response to stress, vesicular trafficking, chemotaxis, and apoptosis (reviewed in Bennett et al., 2006). These actions reflect either binding of PP-IPs to particular protein domains (Ye et al., 1995; Luo et al., 2003) or modification of proteins by phosphorylation (Saiardi et al., 2004).

Intracellular concentrations of PP-IPs are in the submicromolar range in mammalian and yeast cells, but they approach 100–200 μM in slime molds during starvation-induced aggregation (Laussmann et al., 2000). NMR studies of PP-IPs from several species of amoeba reveal the structures of two major PP-IPs, diphosphoinositol pentakisphosphate (PP-IP_5 or IP_7) and bis-diphosphoinositol tetrakisphosphate ($[PP]_2$-IP_4 or IP_8) (Laussmann et al., 1996, 1997, 1998), both of which display variable stereochemistry. In several species of *Dictyostelium*, the most abundant IP_7 isomer (90%) is 6-PP-(1,2,3,4,5)IP_5 (or simply 6-PP-IP_5), and the minor isomer is 5-PP-IP_5, whereas the major IP_8 isomer is 5,6-$[PP]_2$-IP_4 (Laussmann et al., 1998). By contrast, in *Polysphondylium*, 5-PP-IP_5 is the prevalent IP_7 (70%), with 6-PP-IP_5 making up 30%. Besides the major IP_8 isomer 5,6-$[PP]_2$-IP_4 (75%), 25% of IP_8 is 1(3),5-$[PP]_2$-IP_4 (Laussmann et al., 1998). (Enantiomer positions C1/C3 and C4/C6 of the inositol ring cannot be distinguished by NMR. For simplicity, the enantiomer positions are written within brackets, i.e., 1(3),5-$[PP]_2$-IP_4) throughout the text.) While these compounds are all of the *myo* configuration, the only non-*myo* PP-IPs identified to date by NMR are from lysates of *Entamoeba histolytica* (2-PP-*neo*-IP_5, and 2,5-$[PP]_2$-*neo*-IP_4) (Martin et al., 2000). No structures of PP-IPs isolated from mammalian cells have been reported thus far. Chromatographic comparison of the lysates from several mammalian cell lines (Albert et al., 1997) with IP_7 standards suggests that the major IP_7 species is 5-PP-IP_5.

PP-IPs are synthesized mainly from two naturally abundant precursor molecules, *myo*-inositol pentakisphosphate (1,3,4,5,6)IP_5 (IP_5) and *myo*-inositol hexakisphosphate (IP_6) (reviewed in Irvine and Schell, 2001; Shears, 2004). Inositol hexakisphosphate kinase (IP6K) was the first enzyme identified to synthesize PP-IPs from IP_5 and IP_6, by utilizing ATP as a phosphate donor (Voglmaier et al., 1996; Saiardi et al., 1999, 2000, 2001a; Schell et al., 1999). Mammalian cells contain three isoforms of IP6K designated

IP6K1, IP6K2, and IP6K3. Homologs in yeast, named Kcs1 (Saiardi et al., 1999), and in *Dictyostelium* (Luo et al., 2003) have been identified, and a gene encoding IP6K occurs in the genome of the early eukaryote *Giardia* (reviewed in Irvine, 2005). PP-IPs have been found in plants, although no IP6K-like enzyme has yet been identified. In vitro, all mammalian IP6Ks phosphorylate IP_6 to IP_7 and IP_8, and IP_5 to PP-IP_4 and $[PP]_2$-IP_3 (reviewed in Bennett et al., 2006).

IP6Ks belong to the superfamily of inositol phosphate kinases (IPK) (Irvine and Schell, 2001). Another member of the IPK superfamily, inositol phosphate multikinase (IPMK or IPK2), synthesizes PP-IPs from IP_5 (Saiardi et al., 2001b; Zhang et al., 2001; Nalaskowski et al., 2002). In addition, enzymes not related to the IPK superfamily also generate PP-IPs. Recently, the *S. cerevisiae* protein Vip1 (Mulugu et al., 2007) was shown to possess IP_6/IP_7 and (1,2,3,4,5)IP_5-kinase activity, and NMR analyses suggest that IP_7, synthesized by human IP6K1 and yeast Vip1, is 5-PP-IP_5 and 4(6)-PP-IP_5, respectively. Two Vip1-like proteins were found in mammalian cells (Fridy et al., 2007; Choi et al., 2007). Thus, PP-IPs in eukaryotic cells reflect the sum of the activities of at least three families of kinases, IP6Ks, IPMK, and the Vip1-like kinases.

To elucidate the contribution of IP6Ks to the pool of PP-IPs in mammalian cells, we have conducted a detailed structural analysis of the products made by all three IP6Ks from IP_5 and IP_6. We show that the three IP6K isoforms share the same activities both in vivo and in vitro. The promiscuous activity of mammalian IP6Ks leads to products of diverse, yet specific, stereochemistry. A most compelling finding is that IP6K does not only synthesize pyrophosphate bonds, but it also introduces triphosphate groups on both IP_5 and IP_6.

RESULTS

The Activities of All Three IP6K Isoforms Are Similar In Vivo and In Vitro

We compared the catalytic activities of all three mammalian IP6K isoforms in vivo and in vitro. IP6K1, IP6K2, and IP6K3 were individually overexpressed in a mutant strain of *S. cerevisiae* lacking endogenous IP_6 kinase (*kcs1Δ*). The introduction of any IP6K isoform into *kcs1Δ* resulted in the appearance of three new IPs eluting after IP_6, designated IP_7, IP_{8A}, and IP_{8B} (Figure 1A). Elution conditions used in the HPLC analysis resulted in comparable differences in the elution times between IP_6, IP_7, and IP_8, consistent with the subsequent addition of phosphate groups. However, the difference in elution between the peaks for IP_{8A} and IP_{8B} is much smaller, suggesting the existence of IP_8 isomers.

Lysates of wild-type yeast display IP_7 and IP_{8A}, but not IP_{8B} (Figure 1B). When IP6K2 is overexpressed in these cells, the concentration of IP_{8B} is significantly increased (Figure 1B).

The peaks for IP_7 and IP_{8A} synthesized in yeast cells by IP6Ks overlap with the peaks of IPs produced in vitro by IP6K2 (Figure 1A). While no distinct peak for IP_{8B} is detected in vitro, we observe a more polar product, with a retention time suggesting that it possesses one phosphate group more than IP_8, which we designate IP_9 (Figure 1A). This IP can be detected only after prolonged incubation of IP_6 with IP6K. IP_9 has also been observed with in vivo experiments, but only under special labeling conditions (A.S., unpublished data).

vip1Δkcs1Δ yeast were prepared in order to exclude the contribution of both known yeast IP_6/IP_7 kinases, Kcs1 and Vip1. When IP6K1 is overexpressed in these cells, both IP_{8A} and IP_{8B} are formed, in addition to IP_7 (Figure 1C, middle panel). In the case of IP6K2, IP_{8A} and IP_{8B} merge into one peak (IP_8, Figure 1C, bottom panel). Since IP6K2 behaves similarly to IP6K1 and IP6K3 in all other assays (Figure 1), this broad peak is probably due to the impaired column resolution.

To study the in vivo activity of IP6K toward IP_5 as a substrate, all three IP6K isoforms were overexpressed in the double knockout *ipk1Δkcs1Δ* yeast. In addition to the loss of Kcs1, this yeast strain lacks Ipk1, the enzyme that synthesizes IP_6 from (1,3,4,5,6)IP_5 (York et al., 1999), thus allowing the accumulation of IP_5 in these cells (Saiardi et al., 2002). IP6Ks overexpressed under such conditions utilize IP_5 to form three main products of increasing polarity, designated A, B, and C (Figure 1D). Differences in elution times between the products (IP_5 to A, A to B, and B to C) are similar, suggesting a uniform difference in polarity between successive compounds due to the addition of one phosphate group at a time. Peak A is split, similar to IP_{8A}/IP_{8B}, suggesting the presence of two isomers with different stereochemistry. The existence of isomers of the pyrophosphorylated IP_5-derived products (PP-IP_4 or A in this case) has been previously reported (Zhang et al., 2001; Perera et al., 2004). Twin peaks indicating the existence of isomers are also detected for product C, but only in the case of IP6K2 (Figure 1D).

In the experiments described above, radiolabeled IPs were used to determine IP6K activity in vivo and in vitro. Due to the unavailability of ^{3}[H]IP_5, in vitro activities of IP6K isoforms toward IP_5 were determined by using a nonradioactive assay. As described in the following section, the conversion of IP_5 by IP6Ks in vitro is highly comparable with in vivo conditions.

In addition to similar in vivo and in vitro activities of the enzymes, the formation of IP_7 and IP_8, or A, B, and C, is very consistent between independently performed assays. Thus, large-scale in vitro synthesis of IPs for the structural analysis of IP6K products can employ any IP6K isoform.

Development of a Nonradioactive Method Combining HPLC with Inductively Coupled Plasma Mass Spectrometry

Mammalian IP6K1, IP6K2, and IP6K3 were overexpressed in and purified from *E. coli*. The three enzymes were assayed with the nonradiolabeled IP_5 and IP_6. IP6K1 and IP6K2, purified to >95% purity, show comparable activity toward both substrates. IP6K3 exhibits slightly weaker activity (Figures 2A and 2B), which could be due to the limited purity (60%) of the protein.

HPLC based on ion-pair chromatography combined with inductively coupled plasma mass spectrometry (ICP-MS) as the detection system was used to analyze the assay mixtures. ICP-MS was adjusted to continuously detect phosphorus-containing compounds eluted from the column.

With IP_6 as a substrate, IP6Ks consistently produce two peaks, IP_7 and IP_{8A} (Figure 2A), under the assay conditions used in this study. Since IP_{8A} is the only IP_8 isomer in vitro, it is referred to as IP_8 for the rest of the paper.

A time course analysis of product formation by IP6K2 carried out over 4 hr at 37°C reveals almost complete conversion of IP_6 to IP_7 in 20 min (Figure 2C). IP_8 levels increase only after

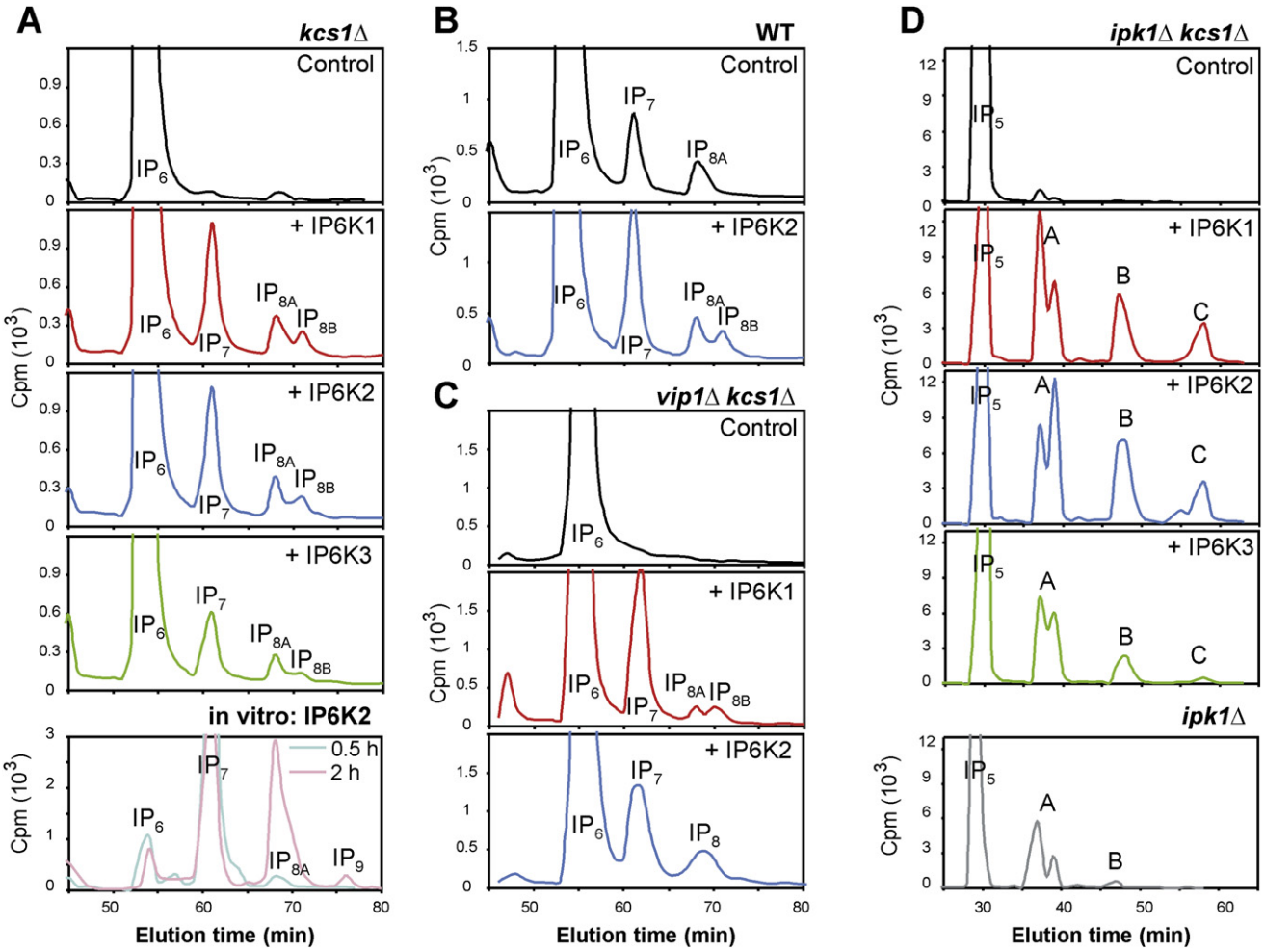

Figure 1. Activity of IP6Ks Overexpressed in Yeast

(A) *kcs1Δ* yeast. Top to bottom: control (empty pADH plasmid); overexpression of IP6K1, IP6K2, and IP6K3; in vitro activity of IP6K2 with IP_6, 0.5 hr and 2 hr assays.

(B) Wild-type (WT) yeast. Top to bottom: control (empty pADH plasmid); overexpression of IP6K2.

(C) *vip1Δkcs1Δ* yeast. Top to bottom: control (empty pADH plasmid); overexpression of IP6K1 and IP6K2.

(D) *ipk1Δkcs1Δ* yeast. Top to bottom: control (empty pADH plasmid); overexpression of IP6K1, IP6K2, and IP6K3; for comparison, *ipk1Δ* yeast. Chromatographic analysis of the radiolabeled IPs on a PartiSphere SAX column is shown.

a significant reduction in the IP_6 concentration, suggesting that IP_8 is formed from the newly synthesized IP_7. Slow synthesis of IP_8 might be due to a higher affinity of the IP6K active site for IP_6 compared with IP_7 as a substrate or to the lower solubility of IP_8 under the assay conditions. A product of higher polarity than IP_8, possibly IP_9, was detected only after prolonged incubation (12 hr or more).

With IP_5 as a substrate, IP6K1 and IP6K2 consistently generate three products with increasing polarity (Figure 2B). IP6K3 forms only the first two products (Figure 2B), most likely due to its generally lower activity. The peaks were assigned as in Figure 1D as A, B, and C. A always elutes as a single peak when using HPLC-ICP-MS, in contrast to the split peak in Figure 1D. As shown later, NMR studies reveal two compounds of similar polarity within peak A. With prolonged assays (beyond 12 hr), we detect two peaks close to the position of peak C (data not shown), resembling the IP6K2 elution profile in Figure 1D.

The time course of product formation by IP6K2 from IP_5 is shown in Figure 2D. Similar to the time course analysis for IP_6, each new product seems to represent a potential substrate for IP6K in another round of phosphorylation.

Partial Inhibition of IP6K Activity by Cacodylate

While screening for the optimal buffer system to be used in IP6K assays, we noticed partial inhibition of IP6K activity with increasing concentrations of cacodylate buffer (data not shown). At 20 mM, the concentration of buffer used in the assays, IP_6 is converted only to IP_7 and IP_5 is converted only to A (Figures 3E and 4B), and the amount of product formed is lower than in Tris buffer (50%–60%). The inhibition is not pH dependent, since the pH of the assay mixtures containing Tris or various concentrations of cacodylate is always in the range in which IP6K is maximally active (i.e., pH 7.5). A separate set of experiments also showed that cacodylate does not inhibit pyruvate kinase/lactate hydrogenase

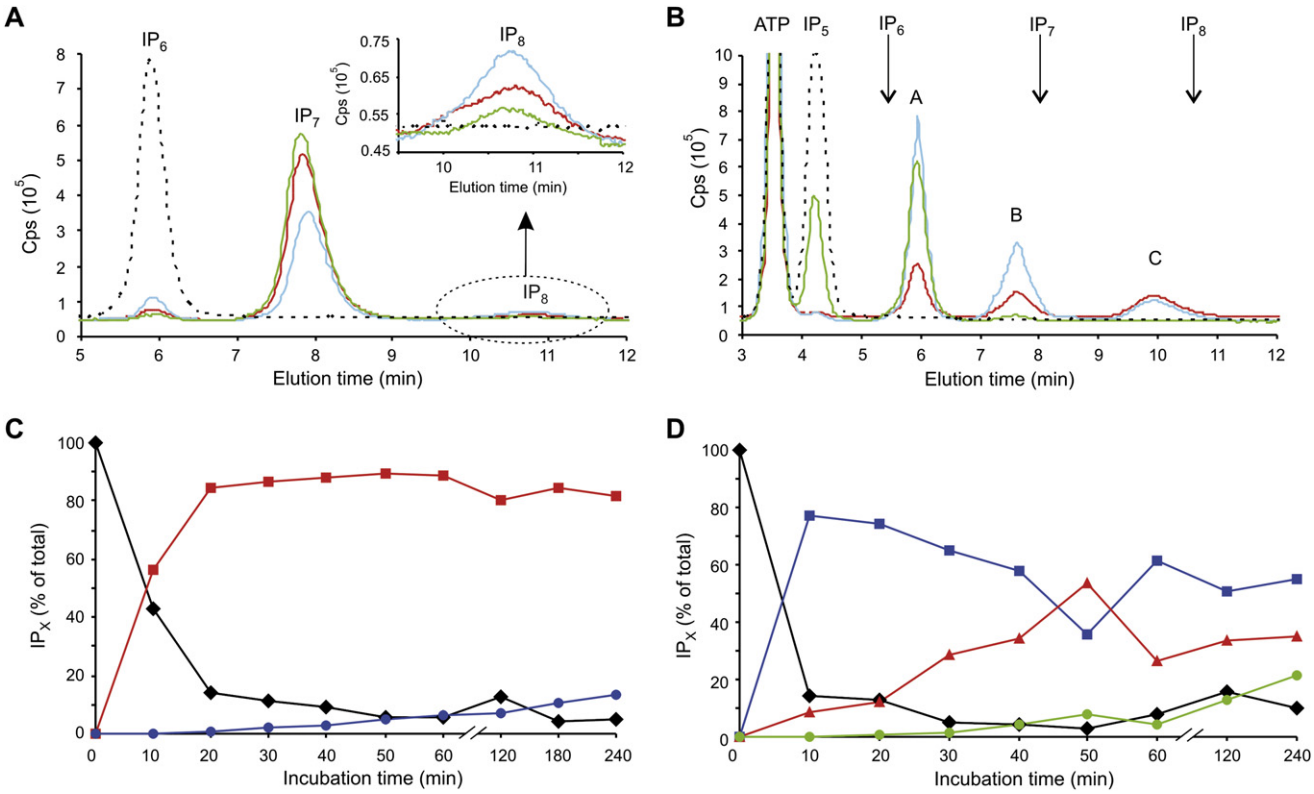

Figure 2. Determination of the In Vitro Activity of IP6K Isoforms by Using a Nonradioactive Method

(A) HPLC-ICP-MS analysis of the IP6K assay mixture with IP_6 (120 μM IP_6, 1 mM $MgCl_2$, 12 hr at 37°C). IP6K1, red; IP6K2, blue; IP6K3, green; control with bovine serum albumin (BSA), black, dashed line. The IP_8 elution profile is enlarged for clarity.

(B) HPLC-ICP-MS analysis of the IP6K assay mixture with IP_5 (250 μM IP_5, 1.5 mM $MgCl_2$, 4 hr at 37°C). IP6K1, red; IP6K2, blue; IP6K3, green; control with BSA, black, dashed line. Elution times for IP_6, IP_7, and IP_8 are marked.

(C) Time course of IP_6 conversion by IP6K2 (120 μM IP_6, 1 mM $MgCl_2$). IP_6, black; IP_7, red; IP_8, blue.

(D) Time course of IP_5 conversion by IP6K2 (250 μM IP_5, 1.5 mM $MgCl_2$). IP_5, black; A, blue; B, red; C, green.

(PK/LDH), used as an ATP-regeneration system in the enzyme assay (data not shown).

This serendipitous discovery of the partial inhibition of IP6K by cacodylate was later used to an advantage in the structural studies of the IP6K products from assay mixtures.

Structural Analysis of Compounds Synthesized by IP6K

The structures of IPs made by IP6K from IP_5 and IP_6 were determined by a combination of NMR and electrospray ionization-mass spectrometry (ESI-MS) (Table 1). All samples analyzed by NMR were adjusted to pH 6.0–6.1. The samples were tested for their integrity throughout sample preparation and after NMR data collection by using HPLC-ICP-MS, and no significant changes over time were seen. The IP structures were determined from ^{1}H-decoupled ^{31}P, ^{1}H-^{31}P Heteronuclear Multiple Bond Correlation with gradients for coherence selection (gHMBC), and ^{1}H-^{1}H Double Quantum Filtered-Correlation Spectroscopy (DQF-COSY) spectra.

NMR spectra crucial for the understanding of IP structure determination are described in the main text. A more detailed presentation of spectra is provided in the Supplemental Data available with this article online.

IP_6 Is Utilized by All Three IP6Ks in the Same Manner to Form IP_7 with a Structure of 5-PP-IP_5

First, HPLC-purified IP_7 produced by IP6K1 was analyzed. ^{1}H-decoupled ^{31}P and ^{1}H-^{31}P gHMBC spectra (Figures 3A and 3C) for pure IP_6 as well as HPLC-purified IP_7 (Figures 3B and 3D) were obtained. In addition, a ^{1}H-^{1}H DQF-COSY spectrum was taken for IP_6 (Figure S1B, see the Supplemental Data).

The pair of doublets in the ^{1}H-decoupled ^{31}P spectrum of IP_7 at −9.0 and −10.2 ppm show the coupling between the α and β phosphorous of the pyrophosphate group in IP_7 (Figure 3B). The peaks with positive values of chemical shifts represent the rest of the inositol ring containing phospho-monoester bonds. Comparison of the ^{1}H-decoupled ^{31}P spectra for IP_6 and IP_7 reveals a shift of the peak for αP5, reflecting pyrophosphorylation at the C5 position of the inositol ring. The shift of the peak representing coupling between H5 and αP5 nuclei is also evident by comparison of the gHMBC spectra of IP_6 and IP_7 (Figures 3C and 3D; ^{1}H-^{31}P gHMBC spectra do not record H/βP coupling). These spectra provide unambiguous evidence that IP6K1 attaches a β-phosphate to the αP5-phosphate group of IP_6. The structure of IP_7 is thus 5-PP-IP_5, as suggested previously from the ^{1}H-decoupled ^{31}P spectrum of IP_7 synthesized by human IP6K1 (Mulugu et al., 2007).

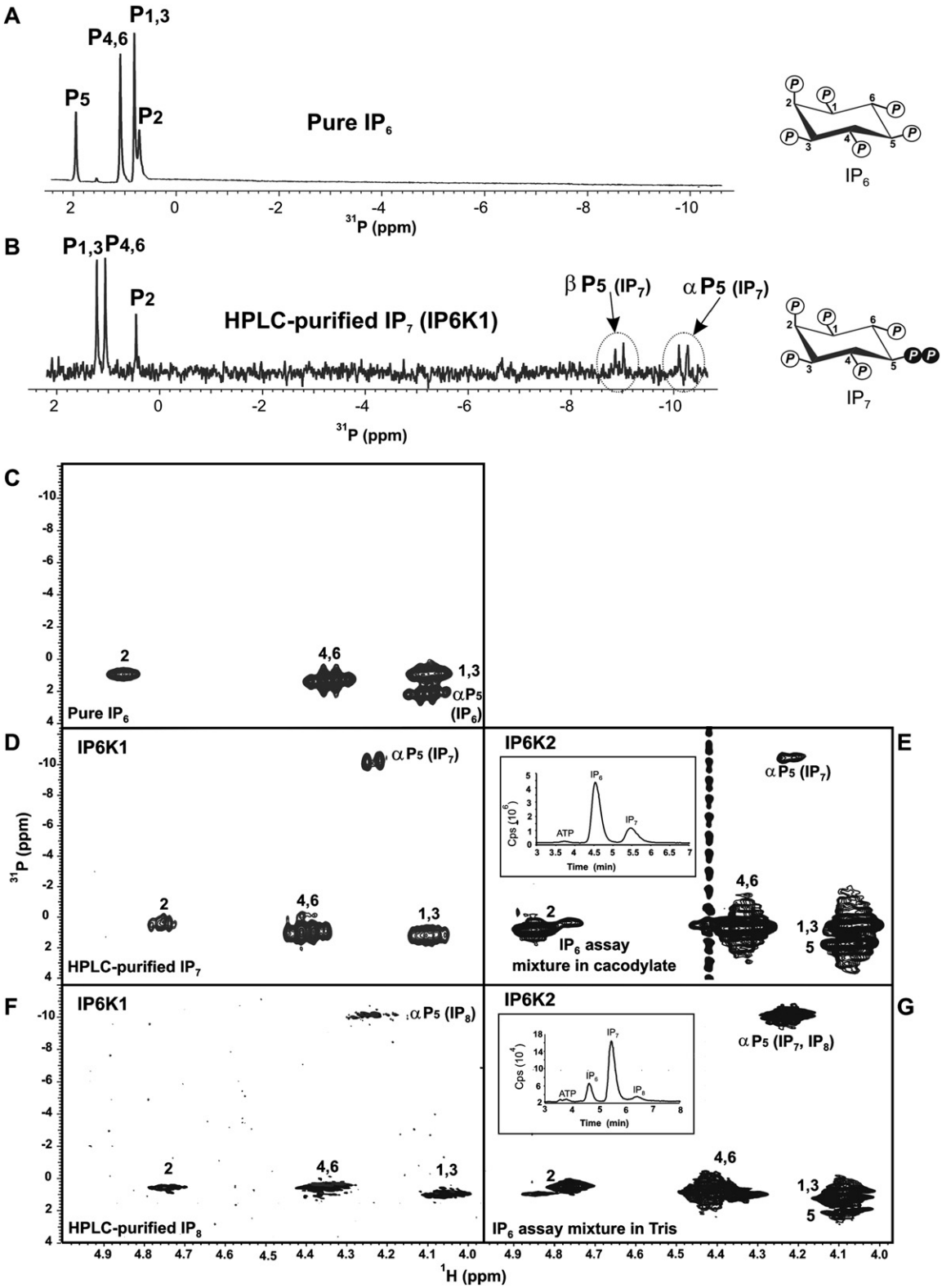

Figure 3. Structures of IP_6 Derivatives Generated by IP6K

(A and B) ^{1}H-decoupled ^{31}P spectrum of (A) pure IP_6 (2 mM) and (B) HPLC-purified IP_7 synthesized by IP6K1 (5-PP-IP_5; 1 mM).
(C–G) ^{1}H-^{31}P gHMBC spectra: the numbers above the peaks mark the positions of the α-phosphate (αP) groups around the inositol ring: (C) Pure IP_6; (D) HPLC-purified IP_7 synthesized by IP6K1; (E) IP_7 synthesized by an IP6K2: assay mixture (12 hr at 37°C) in cacodylate buffer (1 mM IP_6, 0.4 mM IP_7). HPLC-ICP-MS

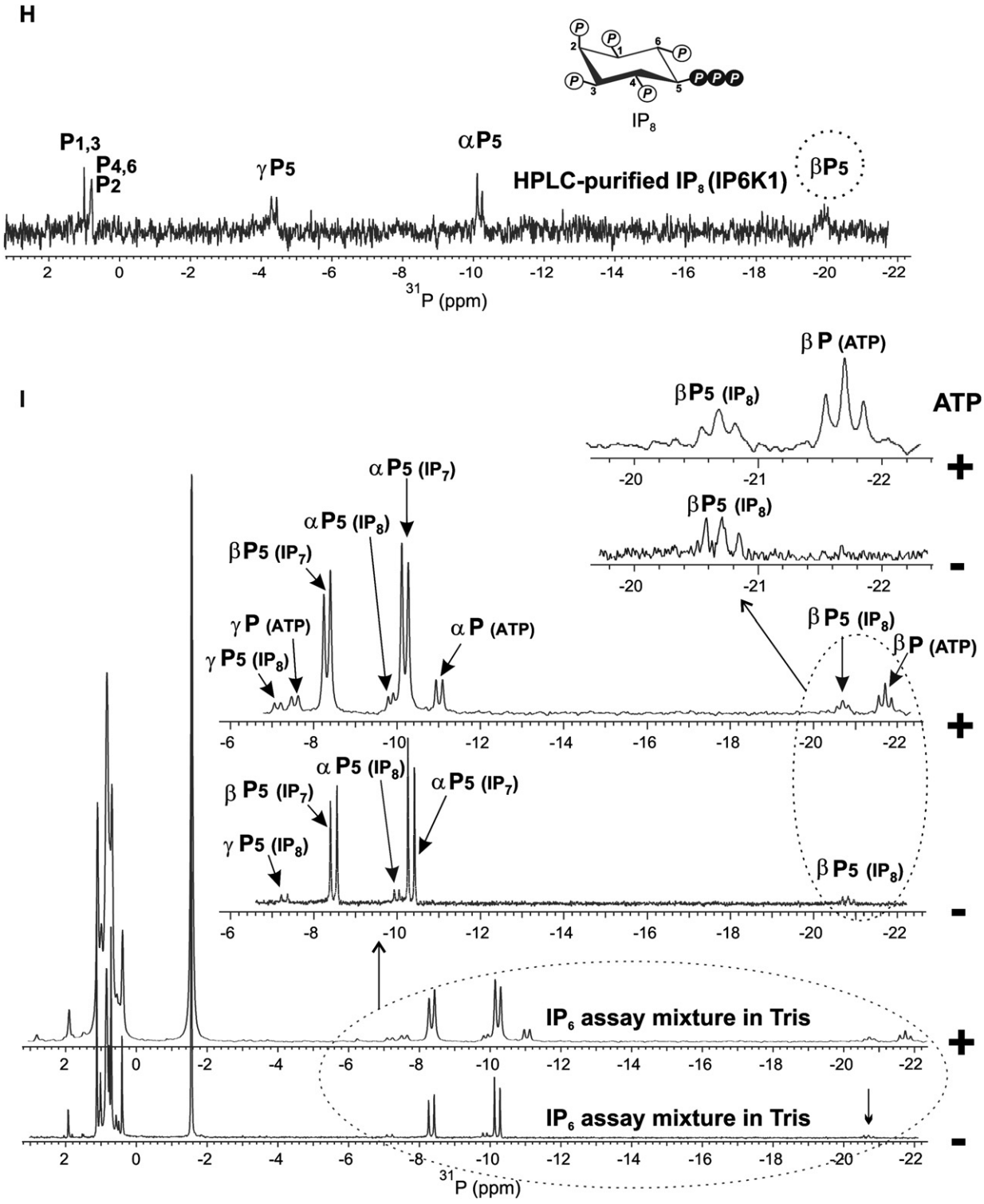

Figure 3. Continued

analysis of the sample is inserted. (F) HPLC-purified IP_8 (0.2 mM) synthesized by IP6K1. (G) IP6K2 assay with IP_6 in Tris buffer (12 hr at 37°C) (0.3 mM IP_6, 1 mM IP_7, 0.1 mM IP_8). HPLC-ICP-MS analysis of the sample is shown in the inset.

(H) ^{1}H-decoupled ^{31}P spectrum of HPLC-purified IP_8 synthesized by IP6K1. The specific position of the multiple peaks belonging to the β-phosphate group of IP_8 triphosphate is marked by a dotted circle.

(I) Bottom: ^{1}H-decoupled ^{31}P spectra of the IP6K2 assay mixture with IP_6 in Tris buffer (the same sample as in [G]), before (−) and after (+) addition of ATP (1.5 mM). Both spectra are magnified twice for better resolution of the peaks describing pyrophosphate (−6 to −12 ppm) and triphosphate (~−21 ppm) groups. Structures of IP_6 and its derivatives are shown; the white and black balls attached to the inositol ring represent the phosphate groups.

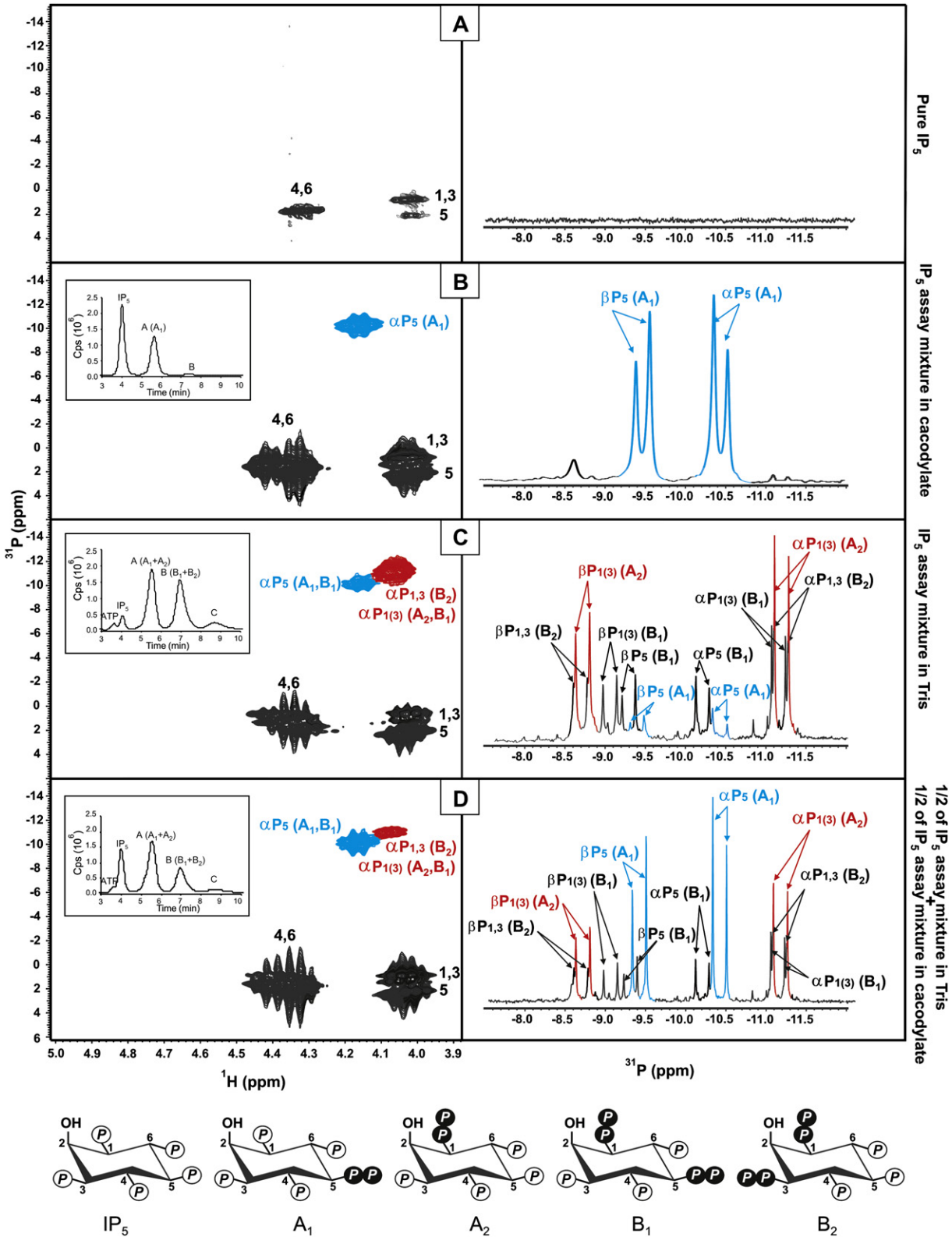

Figure 4. Structures of IP_5 Derivatives Generated by IP6K2

(A) Left: ^{1}H-^{31}P gHMBC spectrum of pure IP_5 (5.2 mM). Right: part of the ^{1}H-decoupled ^{31}P spectrum for comparison with the rest of the spectra in the figure. (B–D) Left: ^{1}H-^{31}P gHMBC spectrum with inserted HPLC-ICP-MS analysis of the sample; right: region on the ^{1}H-decoupled ^{31}P spectrum with peaks describing pyrophosphate groups. (B) Determination of the structure of A_1 (5-PP-IP_4). The IP_5 assay mixture (4 hr at 37°C) in cacodylate buffer (4 mM IP_5, 3 mM A [A_1],

The stereochemistry of IP_7 synthesized by IP6K2 was also determined. To avoid tedious preparation of the large amount of pure IP_7 needed for NMR analysis, the assay mixture was analyzed directly (Figure 3E). The assay was carried out in a cacodylate buffer to prevent the formation of IP_8 and thus reduce the number of compounds contributing to the spectra (Figure 3E). The molecules in the sample containing phosphate groups were phosphoenolpyruvate (PEP), IP_6, and IP_7. Using the information obtained from the spectra of pure IP_6 (Figures 3A and 3C), IP_7 (Figures 3B and 3D), and PEP at pH 6.0 (data not shown), the structure of IP_7 synthesized by IP6K2 was determined to be 5-PP-IP_5.

IP_7 made by IP6K3 was also analyzed by NMR. Due to the lower activity of this isoform, an assay mixture with IP_6 in Tris buffer contained IP_7 as the only product, and its structure was found to be 5-PP-IP_5 (data not shown).

IP_8 Synthesized by IP6Ks from IP_6 Is a Triphosphate: 5-PPP-IP_5

The IP_8 produced by IP6K is a minor species compared with IP_7 (Figures 1 and 2). However, depending on the assay conditions, the conversion of IP_6 to IP_8 in vitro varies from 0% to 30% (Figures 2A and 3G; Figure S5B). NMR spectra were first collected on HPLC-purified IP_8 synthesized by IP6K1 (Figures 3F and 3H). Mass analysis was done with the same sample (Table 1), showing that IP_8 contains two phosphate groups more than IP_6. gHMBC spectra of IP_7 and IP_8 are similar (Figures 3D and 3F), suggesting that IP_8 is a triphosphate since no α-phosphate group other than that of αP5 is additionally phosphorylated. This is also clear from the positions of the peaks in the ^{1}H-decoupled ^{31}P spectrum of IP_8 (Figure 3H). This spectrum contains two doublets at -4.3 ppm and -10.2 ppm, and a multiplet at -20 ppm, assigned as γP5, αP5, and βP5 respectively. Accordingly, IP_8 made by IP6K1 is 5-PPP-IP_5.

Next, we examined the structure of IP_8 synthesized by IP6K2. The IP6K2 assay mixture was prepared in Tris buffer, thus enabling the formation of IP_8 (Figures 3G and 3I). Nucleotides were removed prior to NMR data collection by charcoal treatment. The sample contained IP_6, IP_7, and IP_8; with IP_8 represented $\sim$10% of the mixture (Figures 3G and 3I). The structure of IP_8 made by IP6K2 (5-PPP-IP_5) was extracted with the help of the known spectra for pure IP_6, IP_7, and IP_8. Figure 3I shows the ^{1}H-decoupled ^{31}P spectrum of the mixture, where the multiple peaks (triplet) at -20.7 ppm are assumed to belong to βP5 of IP_8. To ensure that this triplet peak is not due to any remnant ATP, even after charcoal treatment, fresh ATP was added to the sample to a final concentration of 1.5 mM, and another ^{1}H-decoupled ^{31}P spectrum was collected (Figure 3I, ATP [+]). Comparison of spectra before and after the addition of ATP clearly shows that the triplet at -20.7 ppm belongs to the βP of the triphosphate group of IP_8 (5-PPP-IP_5), and that the triplet at -21.7 ppm belongs to the βP of the triphosphate group of ATP. The spectra of a mixture containing higher concentrations of IP_8 (30% of all IPs present) were obtained (Figures S5B and S5C), again confirming the presence of a C5 triphosphate group in IP_8.

With IP6K3, IP_8 could not be obtained in the quantity needed for NMR analysis. Since its IP_8 elutes with the same retention time as IP_8 made by the other two IP6K isoforms (Figure 2A), IP6K3 presumably synthesizes IP_8 of the same structure as synthesized by IP6K1 and IP6K2.

IP_5 Derivatives Synthesized by IP6Ks Contain Pyrophosphate as Well as Triphosphate Groups

Since all three IP6Ks show the same activity toward IP_5 (Figures 1D and 2B), IP6K2 was used as the representative enzyme to synthesize IPs for structural analysis, as it has the highest protein yield. Structures of IP_5 derivatives were determined by using spectra of pure IP_5 and of IP_5 in assay mixtures prepared in cacodylate and in Tris buffer.

The assay mixture prepared in cacodylate buffer contains IP_5 and product A as the only two IPs (Figure 4B). Mass analysis of this sample suggests that A is once-phosphorylated IP_5 derivative (Table 1). A is not IP_6, because the spectra of the IP_5/A mixture (Figure 4B) show no formation of phospho-monoester at the C2 position of IP_5 (no peak for H2/αP2 coupling in the gHMBC spectrum). In addition to peaks for IP_5 (see Figure 4A, left, for comparison), there is, however, a new peak in this spectrum (Figure 4B, left), indicating the presence of a pyrophosphate group, similar to IP_7. The ^{1}H-decoupled ^{31}P spectrum of A obtained by subtraction of the ^{1}H-decoupled ^{31}P spectrum of IP_5 from the corresponding spectrum of the IP_5/A mixture (Figure S7A, peaks in blue) reveals that A contains a pyrophosphate group at the C5 position. The doublets for αP5 and βP5 of A are positioned at -10.5 ppm and -9.5 ppm, respectively (Figure 4B, right). Therefore, A is 5-PP-IP_4.

Spectra of the IP_5 derivatives prepared in Tris buffer are more complex. HPLC-ICP-MS analysis as well as ESI-MS of the sample revealed three compounds of increasing polarity: A with one, B with two, and C with three additional phosphate groups attached to IP_5 (Figure 4C; Table 1). The gHMBC spectrum shows that in the IP_5/A/B/C mixture, the pyrophosphate bonds are present in at least two different positions (Figure 4C). These are C1 (or its enantiomer C3) and C5, based on vertical shifts of the peaks in the gHMBC spectrum relative to the spectra of IP_5 (Figure 4A) and the IP_5/A mixture (Figure 4B). Similar spectra showing the simultaneous presence of pyrophosphate groups at C1(3) and C5 have been determined by Laussmann et al. (1998) for 1(3),5-$[PP]_2$-IP_4 from amoeba. In addition, the highest intensity of the peak in the gHMBC spectrum describing H4(6)/αP4(6) coupling is due to the contribution of the monophosphorylated C4(6) positions of all IPs present within this mixture (Figure 4C).

To determine which peaks in the spectra of the IP_5/A/B/C mixture belong to 5-PP-IP_4, half the volume of the IP_5/A mixture (Figure 4B) was added to half the volume of the IP_5/A/B/C mixture (Figure 4C). The increase in the concentration of 5-PP-IP_4

0.01 mM B). Peaks belonging to αP5 and βP5 of A_1 are in blue. (C) The IP_5 assay mixture (4 hr at 37°C) in Tris buffer (0.6 mM IP_5, 3.5 mM A [A_1+A_2], 2.3 mM B [B_1+B_2], 0.4 mM C). Peaks belonging to αP5/βP5 of A_1 are in blue, and those belonging to αP1(3)/βP1(3) of A_2 are in red. (D) Half the volume of the mixture described in (B) was added to half the volume of the mixture described in (C). The change in the intensity of peaks belonging to A_1 (blue) due to the increased concentration of this compound is evident. The HPLC-ICP-MS analysis of this new mixture is shown in the inset. Determined structures of IP_5 derivatives are depicted. For clarity, 3-PP-IP_4 (A_2 enantiomer) and 3,5-$[PP]_2$-PP_3 (B_1 enantiomer) are not shown.

Table 1. ESI-MS Analysis of IP_5-and IP_6-Derivatives Synthesized by IP6K

Inositol Phosphate	m/z	Molecular Ion Adducts in Positive Mode	Molecular Ion Adducts in Negative Mode
M(**IP_5**)[a] = 580			
MS	579		$[IP_5-H]^-$
M(**A**)[b] = 660			
MS	659		$[A-H]^-$
M(**B**)[b] = 740			
MS	739		$[B-H]^-$
M(**C**)[b] = 820			
MS	819		$[C-H]^-$
M(**IP_6**)[a] = 660			
MS	661	$[IP_6+H]^+$	
M(**IP_7**)[c] = 740			
MS	741	$[IP_7+H]^+$	
M(**IP_8**)[c] = 820			
MS	821	$[IP_8+H]^+$	

[a] Pure IP_5 or IP_6 was used.
[b] The sample used for NMR from the assay mixture prepared in Tris buffer was analyzed (Figure 4C). The same mass for product A was obtained for the NMR sample prepared from the assay mixture in cacodylate buffer (Figure 4B). The mass of the compound that equals the mass of IP_5 plus one phosphate group was assigned to product A, the mass with two extra phosphate groups was assigned to product B, and the mass with three phosphate groups was assigned to product C, according to their increasing retention times in the chromatographic profiles (Figures 1 and 2).
[c] Purified IP_7 or IP_8 was analyzed after NMR (Figure 3). The samples were desalted before ESI-MS analysis.

is reflected in the increased intensity of certain peaks in the spectrum describing this compound (Figure 4D).

The low intensity of the peaks belonging to 5-PP-IP_4 in the original IP_5/A/B/C mixture (Figure 4C) is in contrast to the HPLC-ICP-MS profile of the sample, where A is the major compound. Therefore, the sample must contain another compound of a similar polarity as 5-PP-IP_4, but of a higher concentration. Based on our observation that IP6K also forms pyrophosphate bonds on IP_5 at C1(3), the structure is 1-PP-IP_4 (and/or its enantiomer 3-PP-IP_4). The highest peaks in the one-dimensional spectrum (Figure 4C) therefore belong to 1(3)-PP-IP_4 (also named A_2). 5-PP-IP_4 (also A_1) and A_2 together elute in the highest peak of the HPLC-ICP-MS profile, with A_1 as a minor (20%) and A_2 as a major (80%) fraction.

The HPLC-ICP-MS elution profile (Figure 4C) and mass analysis (Table 1) of the IP_5/A/B/C sample reveal a significant amount of compound B, with two additional phosphate groups attached to IP_5. Since pyrophosphorylation of IP_5 at positions C1 and/or C3 and C5 seems to be favored by IP6K, the structures for B are 1,5-$[PP]_2$-IP_3 (and/or 3,5-$[PP]_2$-IP_3) (B_1) and 1,3-$[PP]_2$-IP_3 (B_2). The peaks corresponding to all of these isomers of B can be assigned in the ^{1}H-decoupled ^{31}P spectrum (Figure 4C; Figure S8). Due to the symmetric structure of B_2, αP1 and αP3 are described with a doublet at −11.2 ppm, and βP1 and βP3 are described with a doublet at −8.7 ppm. Since B_2 is a derivative of A_2, peaks belonging to B_2 pyrophosphate groups almost merge with the corresponding peaks of A_2 (Figure 3C; Figure S8B). B_1 contains pyrophosphate bonds at C1(3) and C5 and can therefore be considered as a "hybrid" of A_1 and A_2. Indeed, the doublet for αP1(3) of B_1 is close to that of αP1(3) of A_2, and the doublet of βP1(3) of B_1 is close to that of βP1(3) of A_2. The doublet for αP5 of B_1 is in close proximity to that of αP5 of A_1, and the doublet for βP5 of B_1 is close to the doublet of βP5 of A_1 (Figure 3C).

Similar to the IP_8 spectrum, a multiplet of peaks in the ^{1}H-decoupled ^{31}P spectrum of the IP_5/A/B/C mixture is present at −22 ppm (Figure S8C). This multiplet consists of at least five peaks, which could represent two merged triphosphate groups, one belonging to ATP and one to an IP compound. Based on the intensity of the multiplet and on mass analysis, this triphosphate group might belong to compounds eluted in peak C, which, besides the triphosphate group, contain a pyrophosphate group at another position on the inositol ring (Figure 4C; Figure S8C; Table 1). Several smaller doublet peaks in the region from −8.5 ppm to −11.5 ppm that could belong to the C isomers support this assumption (Figure 4C; Figure S8C). Interestingly, compound C elutes close to IP_8, which itself is a triphosphate (Figure 2B).

DISCUSSION

IPs containing phospho-anhydride bonds of high energy (PP-IPs) represent a relatively young branch in cell-signaling research. In spite of many, mostly technical, obstacles in the study of these intriguing molecules (Irvine and Schell, 2001; Shears, 2004), knowledge of the evolution and functions of PP-IPs and the enzymes involved in their metabolism has recently developed at an encouraging rate (Bennett et al., 2006; Shears, 2007).

Cells contain structurally diverse, yet nonredundant, PP-IPs, each carrying out their own specific functions (reviewed in Bennett et al., 2006; Shears, 2007). Although the structures of the PP-IPs present in slime molds have been known for some time (Laussmann et al., 1998), information on mammalian PP-IPs has been scarce. To elucidate this missing piece, the main goal of this study has been to determine the structures of PP-IPs synthesized by the mammalian PP-IP synthase, IP6K.

Mammalian IP6K isoforms (IP6K1, IP6K2, IP6K3) share up to 65% amino acid similarity (Saiardi et al., 2001a), which is, as shown here, sufficient for comparable kinase activity both in vivo and in vitro. Differences in their amino acid sequences are mostly confined to the N-terminal halves of the polypeptide chains and to a patch of ~40 residues in the C-terminal half of the protein, following the highly conserved and catalytically important sequence SSLL (Saiardi et al., 2001a). Interestingly, some amino acids from this 40 residue region are responsible for the specific interaction of IP6K2 (but not IP6K1 or IP6K3) with TRAF2 that plays a role in the proapoptotic function of IP6K2 (Morrison et al., 2007). However, only IP6K1 interacts with GRAB, a protein involved in vesicle exocytosis (Luo et al., 2001). These isoform-specific interactions with other proteins seem to be independent of kinase activity. Therefore, whereas the three mammalian IP6Ks synthesize the same panel of PP-IPs, the specificity of function is determined by independent protein-protein-based interactions and by differences in tissue and intracellular distribution between the isoforms.

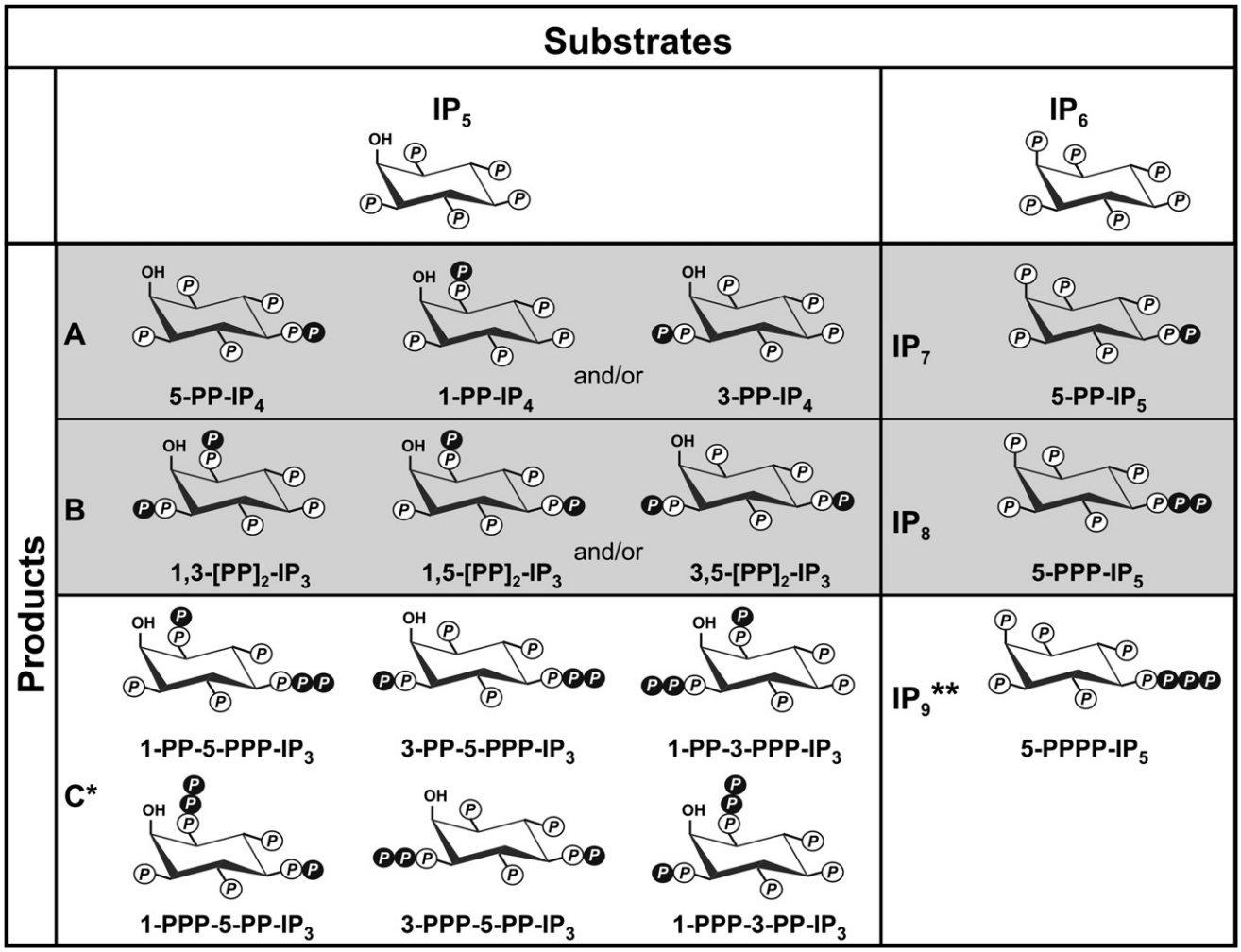

Figure 5. IP_5 and IP_6 Derivatives Synthesized by IP6K

Gray background: structures of products determined in this study (IP_7, IP_8, A, B). White background: C*: proposed structures of IP_5 derivative C (all possible isomers). IP_9**: hypothetical structure of IP_6 derivative IP_9. Phosphate groups added by IP6K to the substrates are marked with black balls.

Figure 5 is summarizing the structural features of PP-IPs synthesized by IP6Ks, as determined in this study. When IP_6 is used as a substrate, IP6K attaches the phosphate group only at the C5 position of the inositol ring, resulting in the formation of 5-PP-IP_5 (IP_7). IP6K can further phosphorylate IP_7 to 5-PPP-IP_5 (IP_8). Chromatographic, mass, and NMR analyses of the IP6K/IP_6 assay mixtures (Figure 3) show that IP_7 is the major product and that IP_8 is the minor product. The ratio between them varies from 90:10 to 70:30 and is similar under both in vivo and in vitro conditions. Our results therefore suggest that 5-PP-IP_5 and 5-PPP-IP_5 are physiologic intracellular products (Figure 1).

The most striking result is that IP_8 synthesized by IP6Ks from IP_6 in vitro is a triphosphoinositol pentakisphosphate (5-PPP-IP_5), and not bis-diphosphoinositol tetrakisphosphate, as suggested previously (reviewed in Bennett et al., 2006). However, 5-PPP-IP_5 is not the only IP_8 isomer made by IP6Ks in cells, as two isomers of IP_8 were detected in vivo (Figures 1A–1C). Mulugu et al. (2007) showed that IP6K converts 4(6)-PP-IP_5, made by the kinase Vip1, to another isomer of IP_8, presumably 4(6),5-$[PP]_2$-IP_4. Although this may be an explanation for the existence of the second (IP_{8B}) isomer in the wild-type and *kcs1Δ* yeast, the existence of the IP_{8B} peak in *vip1Δkcs1Δ* yeast is intriguing (Figures 1A–1C). One possibility is that the yeast genome codes for another IP_6/IP_7 kinase not detected to date. Whereas mammalian cells contain two Vip1-like kinases, only one (Vip1) has been shown thus far in yeast (Mulugu et al., 2007; Fridy et al., 2007; Choi et al., 2007). Another explanation could be that IP6K itself synthesizes the IP_{8B} isoform. A longer incubation time of the in vitro assay shows the formation of the IP_8 (IP_{8A}) peak with a shoulder that overlaps with the IP_{8B} peak (Figure 1A). However, no other IP_8 isoform but 5-PPP-IP_5 was detected in our NMR analyses.

The promiscuity of IP6K's active site reaches yet another level when IP_5 is utilized as a substrate. Under in vitro conditions used in this study, IP6Ks convert IP_5 to several products faster and more consistently than IP_6. The higher solubility of IP_5 and its derivatives compared with IP_6 and its derivatives may contribute to this phenomenon. Substantial conversion of IP_5 also occurs in yeast cells overexpressing IP6K2 (Figure 1D).

Due to experimental limitations, structures of IP_5 derivatives were all determined from the assay mixture by using the deconvolution strategy (Figure 4). The advantage of such a rather complex analysis is that by comparison of the intensity of the peaks belonging to particular IP_5 derivatives we can estimate their ratio in the solution, which cannot be done solely based on chromatographic analysis due to the similar polarity of some of the compounds. Here, we show that IP6K phosphorylates IP_5 at the C1 and/or C3 and C5 positions. The free axial C2-hydroxyl group of IP_5 allows for several different binding modes of IP_5 in the active site of IP6K, at the same time protecting itself from phosphorylation. NMR analysis shows that after 4 hr of incubation at 37°C (Figure 4C), product 1(3)-PP-IP_4 A (A_2) dominates largely over 5-PP-IP_4 (A_1). Products B_1 (1(3),5-$[PP]_2$-IP_3) and B_2 (1,3-$[PP]_2$-IP_3) are made approximately at the same level, although at a lower concentration than A_2 and at a higher concentration than A_1. These structures, together with the data from Figure 2D, suggest that A isomers are formed directly from IP_5, B isomers are formed directly from A, C isomers are formed directly from B, and that the ratio between them varies with time.

Figure 5 also shows structures for the IP_6-or IP_5-derivatives (such as IP_9 and C isomers) that are only hypothetical. These minor products have been detected by chromatographic and/or mass analyses, and they could not be resolved by NMR studies.

The time course for in vitro formation of products by IP6K suggests stepwise phosphorylation events, i.e., when the first product is formed, it is used as a substrate for the formation of a more polar product by the same active site. The phosphorylation sites on the inositol ring determined in our studies (C1, C3, and C5) suggest that the newly formed product must first diffuse out of the active site and later rebind in the mode appropriate for the formation of another pyrophosphate bond at a different position on the inositol ring. The mechanism of formation of the triphosphate group might be more complex, because the elongated polyphosphate chain may make it difficult for the inositol ring to fit into the "typical" (conserved) inositol-binding site. Perhaps there is an additional region in the enzyme that enlarges the conserved inositol-binding domain to enable the triphosphate extension.

Partial inhibition of IP6K by cacodylate is an interesting phenomenon. Chemically, cacodylate is a dimethylarsenate, with a structure that mimics that of phosphate and sulfate ions. Cacodylate has been shown before to bind to the phosphate-binding region of the enzyme's active site (Shenoy et al., 2007). In addition, in the crystal structure of apo-IP3K, sulfate ions (e.g., phosphate analog) were found to bind to the active site and are replaced upon binding of the substrate by its phosphate groups (Gonzalez et al., 2004). Similar competition of cacodylate with IPs and ATP may therefore happen in the active site of IP6K. Another possibility is that cacodylate binds covalently to the serine or cysteine side chains, thereby affecting the activity of the enzyme (Goldgur et al., 1998; Zhu et al., 2003). By binding via either of these two possible modes, cacodylate affects the size and the shape of the IP6K active site. The modified active site now allows IP_5 or IP_6 to bind only in an orientation that leads to pyrophosphorylation at position C5. Binding of IP_5 in an orientation that leads to C1/3 pyrophosphorylation is prohibited. In addition, there is no room in this active site for further phosphorylation to a triphosphate group.

This study demonstrates IP6K's ability to form several diphospho- and triphospho-IP derivatives from IP_5 and IP_6. Furthermore, in vitro as well as in vivo, even more polar peaks than IP_8 can be observed due to IP6K activity. Whether these represent the synthesis of yet another diphosphate group around the ring or even further extension of the existing triphosphate group (i.e., IP_9 with the structure 5-PPPP-IP_5) is unclear. Knowing whether the active site is broad or flexible enough to accommodate different substrates, or if the enzyme uses different phosphorylation mechanisms dependent on the substrates, requires three-dimensional structural analysis of IP6K.

SIGNIFICANCE

IPs are important cellular signaling molecules. Among the many derivatives, the most intriguing are the ones containing highly energetic phospho-anhydride bonds (PP-IPs). Although PP-IPs have been relatively less appreciated by the cell-signaling community, recent information on the synthesis and function of these molecules shows that they may have a wider role in cell physiology than previously understood (Bennett et al., 2006; Shears, 2007). However, information on the structures of these molecules, especially those present in mammalian cells, has been largely missing. Therefore, the main focus of our study was to decipher the structures of PP-IPs synthesized from IP_5 and IP_6 by the three mammalian IP6K isoforms. Our results reveal a group of products derived from both substrates, generated equally by all three IP6K isoforms in vivo and in vitro. These include IP_5-and IP_6-derivatives with pyrophosphate and/or triphosphate groups. The structures of PP-IPs shown in this work can serve as starting points for the elaboration of synthetic PP-IPs by organic chemists, compounds that have been awaited by biologists studying the metabolism and signaling of IPs and PP-IPs. Moreover, since these compounds are involved in many physiologic and pathologic processes (reviewed in Bennett et al., 2006; Shears, 2007; Piccolo et al., 2004; Maffucci et al., 2005), they can also serve as leads for drug discovery or as pharmacological probes of signaling pathways.

EXPERIMENTAL PROCEDURES

Expression of IP6Ks in Yeast and Analysis of IPs

Mammalian IP6Ks were cloned in a high-copy number yeast plasmid, and their expression was driven by the constitutive Alcohol Dehydrogenase (ADH) promoter. The open reading frames (ORFs) for IP6K1, IP6K2, and IP6K3 were obtained by SalI-NotI digestion of pCMV-IP6K1 and pCMV-IP6K2 (Saiardi et al., 1999) and by SalI digestion of pGST-IP6K3 (Saiardi et al., 2001a) and were subcloned in the yeast expression vector pADH. pADH was derived from pYes2NTA (Invitrogen) by substitution of the hexahistidine fusion expression cassette with a GST fusion expression cassette from pGEX4T-2 (GE Healthcare, Sweden) by using PCR and HindIII and PmeI as cloning sites; the Gal4 promoter was subsequently substituted by the ADH promoter obtained by genomic PCR, by using SpeI and HindIII as cloning sites. Plasmids were transformed into *kcs1Δ* and *ipk1Δkcs1Δ S. cerevisiae* derived from the BY4741 parent strain (Saiardi et al., 2002). *vip1Δkcs1Δ* double mutant yeast (parental strain DDY1810) were generated by using standard homologous recombination techniques (Güldener et al., 1996, 2002).

HPLC analysis of IPs was performed as previously described (Azevedo and Saiardi, 2006) (for a detailed description, see the Supplemental Data). Preparation of recombinant IP6Ks from *E. coli* and enzyme assays (radioactive and nonradioactive) are also described in the Supplemental Data.

HPLC-ICP-MS Analysis

HPLC-ICP-MS analysis of the nonradioactive samples was carried out by using reversed-phase ion-pairing chromatography on a Zorbax Eclipse XDB-C8 column (2.1 × 100 mm, 3.5 μm) at 0.2 ml/min. Isocratic elution was performed by using a mixture of 40%–50% Buffer A (20 mM di-ammonium hydrogen citrate, 1.5 mM tetra-butyl-ammonium hydroxide (TBAH), and 2% [v/v] methanol) and 60%–50% Buffer B (20 mM di-ammonium hydrogen citrate, 1.5 mM TBAH, and 16% [v/v] methanol) on an Agilent 1100 series HPLC to give reasonable resolution between the peaks. Buffers A and B were adjusted to pH 6.0 by the addition of 1 M ammonia solution. The column was connected to the Agilent 4500 ICP-MS, where the phosphorus signal at m/z ratio 31 was recorded.

NMR Analysis

Preparation of the samples is described in the Supplemental Data. Samples were transferred either into regular or Shigemi 5 mm diameter NMR tubes. All NMR spectra were acquired at 283K by using the Unity Inova Varian 300 MHz system equipped with a 5 mm Indirect Detection Pulsed Field Gradient probe and an Automation Triple Resonance Broadband probe. ^{1}H chemical shifts were referenced to water (4.80 ppm), and ^{31}P chemical shifts were referenced to external phosphoric acid (0 ppm). Spectra were processed and analyzed by using VNMR 2.1B (VARIAN, Inc.) software.

For ^{1}H-decoupled ^{31}P spectra, 90 degree excitation pulses of 7.6 μs and recovery delays of 1 s were employed, with 32,768 complex points and a spectral width of 13.5 kHz, resulting in digital resolution of 0.4 Hz/point. For ^{1}H decoupling, the WALTZ-16 technique was employed. The number of transients was 8000.

^{1}H-^{31}P gHMBC spectra were recorded with 4096 complex points in the t_2 dimension, 256 increments in the t_1 dimension, and a spectral width of 3.5 kHz in F2 and 5.3 kHz in F1. The number of transients per free induction decay was 320. Recovery delay between experiments was 1.5 s. Appropriate delays were calculated from $^{n}J_{PH}$ = 7.7 Hz.

Assignment of spectra was based on detailed analysis of spectral features and correlations between ^{1}H-decoupled ^{31}P and gHMBC NMR experiments. Individual resonances were assigned on the basis of their chemical shifts, signal intensities, and the multiplicity of resonances.

All NMR data were collected at the Slovenian NMR Centre at the National Institute of Chemistry Slovenia.

Mass Analysis

The mass analysis experiments were conducted on an ion trap LCQ MS system (Finnigan, MAT, San Jose, CA, USA). Mass spectra were recorded with direct injection (20 μl/min) of the sample with a makeup flow of 80% (v/v) methanol in water at 0.2 ml/min. ESI-MS in positive or negative polarity mode was used. The transfer capillary temperature was 200°C, source voltage was 4.0 kV, and sheath gas pressure was 345 kPa.

SUPPLEMENTAL DATA

Supplemental Data include Supplemental Experimental Procedures, NMR spectra in an enlarged format with detailed peak assignments, and DQF-COSY NMR spectra and are available at http://www.chembiol.com/cgi/content/full/15/3/274/DC1/.

ACKNOWLEDGMENTS

We acknowledge expert assistance from Aleksandar Gaćeša, Primož Šket, Mirko Cevec, Maja Capuder, and Boštjan Japelj. This work was supported by grants from the Slovenian Research Agency J4-6463 (M.P.), P1-0034 (M.K.), and 3311-04-831035 (P.D.); by Marie Curie International Re-Integration Grants No. 014882 (M.P.) and 014827 (A.S.); and by Medical Research Council funding of the Cell Biology Unit (A.S.).

Received: August 2, 2007
Revised: December 7, 2007
Accepted: January 23, 2008
Published: March 21, 2008

REFERENCES

Albert, C., Safrany, S.T., Bembenek, M.E., Reddy, K.M., Reddy, K.K., Falck, J.R., Brocker, M., Shears, S.B., and Mayr, G.W. (1997). Biological variability in the structures of diphosphoinositol polyphosphates in *Dictyostelium discoideum* and mammalian cells. Biochem. J. *327*, 553–560.

Azevedo, C., and Saiardi, A. (2006). Extraction and analysis of soluble inositol polyphosphates from yeast. Nat. Protoc. *1*, 2416–2422.

Bennett, M., Onnebo, S.M.N., Azevedo, C., and Saiardi, A. (2006). Inositol pyrophosphates: metabolism and signaling. Cell. Mol. Life Sci. *63*, 552–564.

Choi, J.H., Williams, J., Cho, J., Falck, J.R., and Shears, S.B. (2007). Purification, sequencing, and molecular identification of a mammalian PP-InsP(5) kinase that is activated when cells are exposed to hyperosmotic stress. J. Biol. Chem. *282*, 30763–30775.

Fridy, P.C., Otto, J.C., Dollins, D.E., and York, J.D. (2007). Cloning and characterization of two human VIP1-like inositol hexakisphosphate and diphosphoinositol pentakisphosphate kinases. J. Biol. Chem. *282*, 30754–30762.

Glennon, M.C., and Shears, S.B. (1993). Turnover of inositol pentakisphosphates, inositol hexakisphosphate and diphosphoinositol polyphosphates in primary cultured-hepatocytes. Biochem. J. *293*, 583–590.

Goldgur, Y., Dyda, F., Hickman, A.B., Jenkins, T.M., Craigie, R., and Davies, D.R. (1998). Three new structures of the core domain of HIV-1 integrase: an active site that binds magnesium. Proc. Natl. Acad. Sci. USA *95*, 9150–9154.

Gonzalez, B., Schell, M.J., Letcher, A.J., Veprintsev, D.B., Irvine, R.F., and Williams, R.L. (2004). Structure of a human inositol 1,4,5-trisphosphate 3-kinase: substrate binding reveals why it is not a phosphoinositide 3-kinase. Mol. Cell *15*, 689–701.

Güldener, U., Heck, S., Fiedler, T., Beinhauer, J., and Hegemann, J.H. (1996). A new efficient gene disruption cassette for repeated use in budding yeast. Nucleic Acids Res. *24*, 2519–2524.

Güldener, U., Heinisch, J., Köhler, G.J., Voss, D., and Hegemann, J.H. (2002). A second set of loxP marker cassettes for Cre-mediated multiple gene knockouts in budding yeast. Nucleic Acids Res. *30*, e23.

Hand, C.E., and Honek, J.F. (2007). Phosphate transfer from inositol pyrophosphates InsP(5)PP and InsP(4)(PP)(2): a semi-empirical investigation. Bioorg. Med. Chem. Lett. *17*, 183–188.

Irvine, R.F. (2005). Inositide evolution - towards turtle domination? J. Physiol. *566*, 295–300.

Irvine, R.F., and Schell, M.J. (2001). Back in the water: the return of the inositol phosphates. Nat. Rev. Mol. Cell Biol. *2*, 327–338.

Laussmann, T., Eujen, R., Weisshuhn, C.M., Thiel, U., and Vogel, G. (1996). Structures of diphospho-myo-inositol pentakisphosphate and bisdiphospho-myo-inositol tetrakisphosphate from *Dictyostelium* resolved by NMR analysis. Biochem. J. *315*, 715–720.

Laussmann, T., Reddy, K.M., Reddy, K.K., Falck, J.R., and Vogel, G. (1997). Diphospho-myo-inositol phosphates from *Dictyostelium* identified as D-6-diphospho-myo-inositol pentakisphosphate and D-5,6-bisdiphospho-myo-inositol tetrakisphosphate. Biochem. J. *322*, 31–33.

Laussmann, T., Hansen, A., Reddy, K.M., Reddy, K.K., Falck, J.R., and Vogel, G. (1998). Diphospho-myo-inositol phosphates in *Dictyostelium* and *Polysphondylium*: identification of a new bisdiphospho-myo-inositol tetrakisphosphate. FEBS Lett. *426*, 145–150.

Laussmann, T., Pikzack, C., Thiel, U., Mayr, G.W., and Vogel, G. (2000). Diphospho-myo-inositol phosphates during the life cycle of *Dictyostelium* and *Polysphondylium*. Eur. J. Biochem. *267*, 2447–2451.

Luo, H.R., Saiardi, A., Nagata, E., Ye, K.Q., Yu, H.B., Jung, T.S., Luo, X.J., Jain, S., Sawa, A., and Snyder, S.H. (2001). GRAB: a physiologic guanine nucleotide exchange factor for Rab3A, which interacts with inositol hexakisphosphate kinase. Neuron *31*, 439–451.

Luo, H.R., Huang, Y.E., Chen, J.M.C., Saiardi, A., Iijima, M., Ye, K.Q., Huang, Y.F., Nagata, E., Devreotes, P., and Snyder, S.H. (2003). Inositol pyrophosphates mediate chemotaxis in *Dictyostelium* via pleckstrin homology domain-PtdIns (3,4,5)P3 interactions. Cell *114*, 559–572.

Maffucci, T., Piccolo, E., Cumashi, A., Iezzi, M., Riley, A.M., Saiardi, A., Godage, H.Y., Rossi, C., Broggini, M., Iacobelli, S., et al. (2005). Inhibition of the phosphatidylinositol 3-kinase/Akt pathway by inositol pentakisphosphate results in antiangiogenic and antitumor effects. Cancer Res. *65*, 8339–8349.

Martin, J.B., Laussmann, T., Bakker-Grunwald, T., Vogel, G., and Klein, G. (2000). neo-Inositol polyphosphates in the amoeba *Entamoeba histolytica*. J. Biol. Chem. *275*, 10134–10140.

Menniti, F.S., Miller, R.N., Putney, J.W., and Shears, S.B. (1993a). Turnover of inositol polyphosphate pyrophosphates in pancreatoma cells. J. Biol. Chem. *268*, 3850–3856.

Menniti, F.S., Oliver, K.G., Putney, J.W., and Shears, S.B. (1993b). Inositol phosphates and cell signaling - new views of Insp5 and Insp6. Trends Biochem. Sci. *18*, 53–56.

Michell, R.H. (2007). Evolution of the diverse biological roles of inositols. Biochem. Soc. Symp. *74*, 223–246.

Morrison, B.H., Bauer, J.A., Lupica, J.A., Tang, Z., Schmidt, H., DiDonato, J.A., and Lindner, D.J. (2007). Effect of inositol hexakisphosphate kinase 2 on transforming growth factor β-activated kinase 1 and NF-κ B activation. J. Biol. Chem. *282*, 15349–15356.

Mulugu, S., Bai, W.L., Fridy, P.C., Bastidas, R.J., Otto, J.C., Dollins, D.E., Haystead, T.A., Ribeiro, A.A., and York, J.D. (2007). A conserved family of enzymes that phosphorylate inositol hexakisphosphate. Science *316*, 106–109.

Nalaskowski, M.M., Deschermeier, C., Fanick, W., and Mayr, G.W. (2002). The human homologue of yeast ArgRIII protein is an inositol phosphate multikinase with predominantly nuclear localization. Biochem. J. *366*, 549–556.

Perera, N.M., Michell, R.H., and Dove, S.K. (2004). Hypo-osmotic stress activates Plc1p-dependent phosphatidylinositol 4,5-bisphosphate hydrolysis and inositol hexakisphosphate accumulation in yeast. J. Biol. Chem. *279*, 5216–5226.

Piccolo, E., Vignati, S., Maffucci, T., Innominato, P.F., Riley, A.M., Potter, B.V.L., Pandolfi, P.P., Broggini, M., Iacobelli, S., Innocenti, P., et al. (2004). Inositol pentakisphosphate promotes apoptosis through the PI3-K/Akt pathway. Oncogene *23*, 1754–1765.

Saiardi, A., Erdjument-Bromage, H., Snowman, A.M., Tempst, P., and Snyder, S.H. (1999). Synthesis of diphosphoinositol pentakisphosphate by a newly identified family of higher inositol polyphosphate kinases. Curr. Biol. *9*, 1323–1326.

Saiardi, A., Caffrey, J.J., Snyder, S.H., and Shears, S.B. (2000). The inositol hexakisphosphate kinase family - catalytic flexibility and function in yeast vacuole biogenesis. J. Biol. Chem. *275*, 24686–24692.

Saiardi, A., Nagata, E., Luo, H.R., Snowman, A.M., and Snyder, S.H. (2001a). Identification and characterization of a novel inositol hexakisphosphate kinase. J. Biol. Chem. *276*, 39179–39185.

Saiardi, A., Nagata, E., Luo, H.B.R., Sawa, A., Luo, X.J., Snowman, A.M., and Snyder, S.H. (2001b). Mammalian inositol polyphosphate multikinase synthesizes inositol 1,4,5-trisphosphate and an inositol pyrophosphate. Proc. Natl. Acad. Sci. USA *98*, 2306–2311.

Saiardi, A., Sciambi, C., McCaffery, J.M., Wendland, B., and Snyder, S.H. (2002). Inositol pyrophosphates regulate endocytic trafficking. Proc. Natl. Acad. Sci. USA *99*, 14206–14211.

Saiardi, A., Bhandari, R., Resnick, A.C., Snowman, A.M., and Snyder, S.H. (2004). Phosphorylation of proteins by inositol pyrophosphates. Science *306*, 2101–2105.

Schell, M.J., Letcher, A.J., Brearley, C.A., Biber, J., Murer, H., and Irvine, R.F. (1999). PiUS (Pi uptake stimulator) is an inositol hexakisphosphate kinase. FEBS Lett. *461*, 169–172.

Shears, S.B. (2004). How versatile are inositol phosphate kinases? Biochem. J. *377*, 265–280.

Shears, S.B. (2007). Understanding the biological significance of diphosphoinositol polyphosphates ('inositol phosphates'). Biochem. Soc. Symp. *74*, 211–221.

Shenoy, A.R., Capuder, M., Draskovic, P., Lamba, D., Visweswariah, S.S., and Podobnik, M. (2007). Structural and biochemical analysis of the Rv0805 cyclic nucleotide phosphodiesterase from *Mycobacterium tuberculosis*. J. Mol. Biol. *365*, 211–225.

Stephens, L., Radenberg, T., Thiel, U., Vogel, G., Khoo, K.H., Dell, A., Jackson, T.R., Hawkins, P.T., and Mayr, G.W. (1993). The detection, purification, structural characterization, and metabolism of diphosphoinositol pentakisphosphate(S) and bisdiphosphoinositol tetrakisphosphate(S). J. Biol. Chem. *268*, 4009–4015.

Streb, H., Irvine, R.F., Berridge, M.J., and Schulz, I. (1983). Release of Ca-2+ from a nonmitochondrial intracellular store in pancreatic acinar-cells by inositol-1,4,5-trisphosphate. Nature *306*, 67–69.

Voglmaier, S.M., Bembenek, M.E., Kaplin, A.I., Dorman, G., Olszewski, J.D., Prestwich, G.D., and Snyder, S.H. (1996). Purified inositol hexakisphosphate kinase is an ATP synthase: diphosphoinositol pentakisphosphate as a high-energy phosphate donor. Proc. Natl. Acad. Sci. USA *93*, 4305–4310.

Ye, W., Ali, N., Bembenek, M.E., Shears, S.B., and Lafer, E.M. (1995). Inhibition of clathrin assembly by high-affinity binding of specific inositol polyphosphates to the synapse-specific clathrin assembly protein Ap-3. J. Biol. Chem. *270*, 1564–1568.

York, J.D., Odom, A.R., Murphy, R., Ives, E.B., and Wente, S.R. (1999). A phospholipase C-dependent inositol polyphosphate kinase pathway required for efficient messenger RNA export. Science *285*, 96–100.

Zhang, T., Caffrey, J.J., and Shears, S.B. (2001). The transcriptional regulator, Arg82, is a hybrid kinase with both monophosphoinositol and diphosphoinositol polyphosphate synthase activity. FEBS Lett. *494*, 208–212.

Zhu, X., Larsen, N.A., Basran, A., Bruce, N.C., and Wilson, I.A. (2003). Observation of an arsenic adduct in an acetyl esterase crystal structure. J. Biol. Chem. *278*, 2008–2014.

